ORIGINAL ARTICLE

Silicate Profiles Characterization in Lateritic Nickel Deposit of Punta Gorda, Moa, Cuba

Caracterización de perfiles silicatados en el depósito laterítico de níquel de Punta Gorda, Moa, Cuba

Arturo Luis Rojas-Purón[1]*, Rômulo Simões-Angélica[2], Lázaro Fernández-Martínez[3], Andres Salazar-Moreno[1]

[1]University of Moa, Holguín, Cuba.

[2]Federal University of Pará, Belem, Brasil.

[3]Níquel and Cobalt Producing Company *Ernesto Che Guevara*, Moa, Holguín, Cuba.

*Correspondance´Author: arojaspurnh@gmail.com

Abstract

Although the lateritic profiles of Punta Gorda deposit, Moa municipality have been classified as oxidized, studies related to the quality of nickel ore have revealed within the deposit, sectors with clayey and smectite type profiles. This prompted the mineralogical characterization of the saprolitic horizons of the lateritic profiles in the O-48 block of the deposit, with X-ray diffraction and ICP-AES spectroscopy techniques. Lateritic profiles constituted by clay horizons (with predominance of kaolinite) associated with smectitic-chloritic horizons were distinguished. Smectite are Fe- saponite and montmorillonite type and the chlorites of the clinochlorite type, enriched in Fe. The paragenesis of the smectite (Sm)-chloritic (Chl) component is interpreted as a process of progressive weathering from Sm to Chl. In the O-48 sector of the Punta Gorda deposit, the smectitic-chloritic saprolite are the carriers of highest amount of nickel, with contents from 1.07 % to 1.59 % NiO, while the kaolinite ones are poor in this metal (less than 0.69 % NiO).

Keywords: ferrous nickeliferous laterites, nickel ores, weathering crusts, Punta Gorda deposit, kaolinite, chlorites, smectite, goethite

Resumen

Aunque los perfiles lateríticos del yacimiento Punta Gorda (Moa) han sido clasificados como oxidados, estudios relativos a la calidad de la mena niquelífera han revelado dentro del yacimiento sectores con perfiles del tipo arcilloso y esmectítico. Ello incitó a caracterizar mineralógicamente los horizontes saprolíticos de los perfiles lateríticos en el bloque O-48 del

yacimiento, con técnicas de Difracción de rayos-X y Espectroscopía de ICP-AES. Se distinguieron de este modo, perfiles lateríticos constituidos por horizontes propiamente arcillosos (con predominio de caolinita) asociados con perfiles de horizontes esmectíticos–cloríticos. Las esmectitas son del tipo saponita-Fe y montmorillonita y las cloritas del tipo clinocloro, enriquecidas en Fe. La paragénesis del componente esmectítico (Sm)- clorítico (Chl) se interpreta como un proceso de meteorización progresiva de Sm a Chl. En el sector O-48 del depósito Punta Gorda, las saprolitas esmectíticas–cloríticas son las portadoras de la mayor cantidad de níquel, con contenidos desde 1,07 % hasta 1,59 % de NiO, mientras que las caoliníticas son pobres en este metal (menos de 0,69 % de NiO).

Palabras clave: lateritas ferroniquelíferas, menas de níquel, cortezas de meteorización, depósito Punta Gorda, caolinita, cloritas, esmectitas, goethita, níquel

1. INTRODUCCIÓN

Based on the mineralogy of the predominant ore, Ni-Co lateritic deposits are classified into three types: a) hydrous silicate-type deposits, b) oxide-type deposits, and c) clay-type deposits (Brand *et al.*, 1998; Elias, 2002; Gleeson *et al.*, 2003; Freyssinnet *et al.*, 2005).

Cuban Ni-Co lateritic deposits are predominantly of the oxide type, among which is the Punta Gorda deposit (Brand *et al.*, 1998; Gleeson *et al.*, 2003; Marsh and Anderson, 2011; Butt and Cluzel, 2013; Domenech *et al.*, 2017). From a geological perspective, the deposit is situated within the Moa-Baracoa ophiolitic massif, which is composed of oceanic units from the Mayarí-Baracoa ophiolitic belt, located in northeastern Cuba (Iturralde-Vinent, 1996; Proenza *et al.*, 1999).

The Moa-Baracoa massif (Figure 1A) consists of a harzburgitic tectonite mantle, with subordinate dunite, and a remarkably well-preserved Moho Transition Zone (MTZ) (Figure 1B). The MTZ contains stratified and isotropic gabbros and pillow basalts, which are overlain by mantle sequences (Marchesi *et al.*, 2006). The ultramafic rocks are serpentinized up to 95% relative to typical serpentinite. The peridotites are cross-cut by dikes of gabbro, pegmatitic gabbro, olivine norite, and minor pyroxenite (Proenza *et al.*, 1999; Marchesi *et al.*, 2006).Los depósitos lateríticos de Ni-Co, atendiendo a la mineralogía de la mena predominante, se clasifican en tres tipos: a) depósitos de tipo silicatado hidratado, b) depósitos de tipo óxido y c) depósitos de tipo arcilla (Brand *et al.*, 1998; Elias, 2002; Gleeson *et al.*, 2003; Freyssinnet *et al.*, 2005).

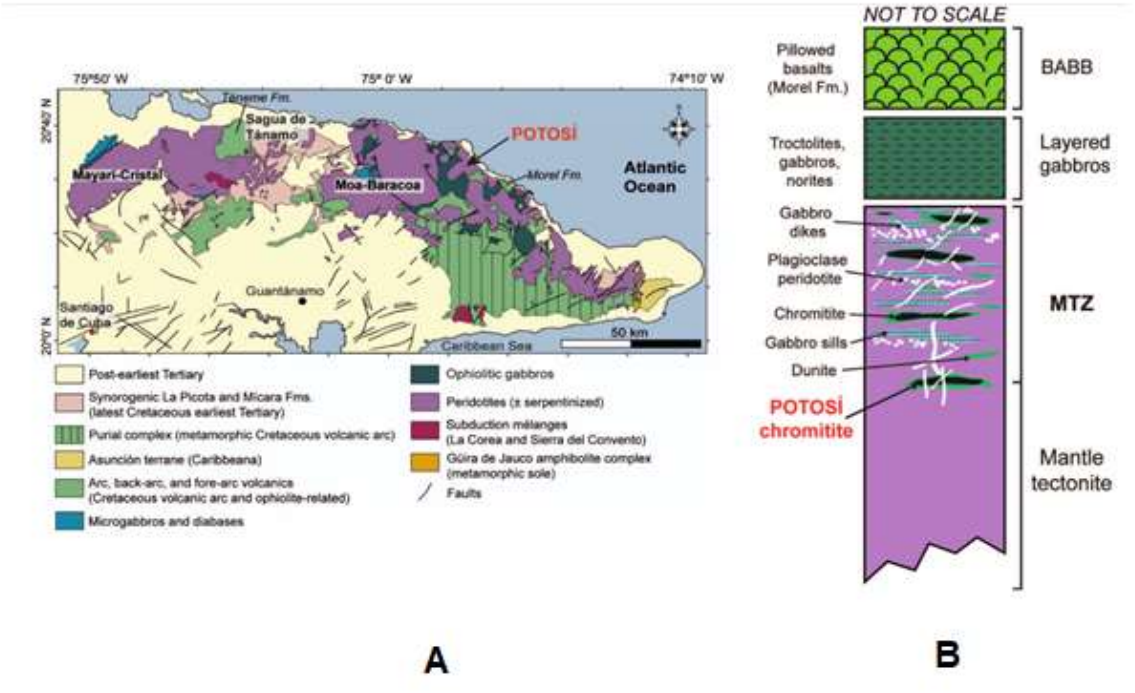

Figure 1. A) Regional geological map of the Eastern Cuban Northeastern Ophiolitic Massifs, modified from Pushcharovsky *et al.* (1988). B) Lithostratigraphic column schematic of the Moa-Baracoa Ophiolitic Massif, modified from Marchesi *et al.* (2006).

The nickel lateritic crusts of Punta Gorda have developed from the weathering of ultramafic rocks (primarily harzburgites and, to a lesser extent, dunites) and mafic rocks of the ophiolitic massif, which includes gabbro bodies.

From a mineralogical standpoint, the deposit has been studied as a typical ferronickel crust composed of oxidized lateritic profiles (Lavaut-Copa, 1998; Lavaut-Copa, 2018; Oliveira *et al.*, 2001; Galí *et al.*, 2006; Rojas *et al.*, 2012; Domenech *et al.*, 2017; Aiglsperger *et al.*, 2016). A notable characteristic is the presence, in the upper horizons of the regolithic unit, of Fe oxides (goethite, hematite, maghemite), Mn oxyhydroxides (asbolane, lithiophorite), and Al oxyhydroxides (gibbsite) intermixed with Fe-Mg silicates (serpentine, chlorites, pyroxenes), among other minerals.

The Punta Gorda deposit is currently being mined by the "Empresa Productora de Níquel Ernesto Che Guevara," which utilizes the carbonate-ammonia technology (known as the Caron process) to produce nickel oxide. Studies concerning the quality of the ore feed for this process (Terrero-Reynosa, 2010; Fernández-Martínez, 2020) have revealed the existence of atypical sectors within the deposit (particularly in block O-48), characterized by the presence of clays mixed with other silicates.

The discovery of these atypical sectors suggests the potential presence of large bodies or stratigraphic units related to the mantle-crust transition zone (Proenza *et al.*, 1999). This would explain the occurrence of clay and other minerals in areas proximal to the deposit and their relationship with more basic protoliths (feldspars, Al-rich pyroxenes, etc.) that generate clayey or smectitic profiles.

The foregoing rationale motivated a research initiative aimed at characterizing the mineralogy of the saprolitic horizons within the lateritic profiles of block O-48 at the Punta Gorda deposit. The primary objective was to determine the existence of non-oxidized profiles in this area.

2. MATERIALS AND METHODS

The investigation was conducted in the O-48 sector (Figure 2), which encompasses an approximate outcrop area of 60 m² within the Punta Gorda deposit. This deposit has developed upon a basement of serpentinized ultrabasic and basic rocks, which exhibits evidence of petrological diversity that may include bodies of gabbros and basalts (Marchesi *et al.*, 2006), as well as peridotites cross-cut by dikes of gabbro, olivine norites, and pyroxenites (Terrero-Reynosa, 2010).

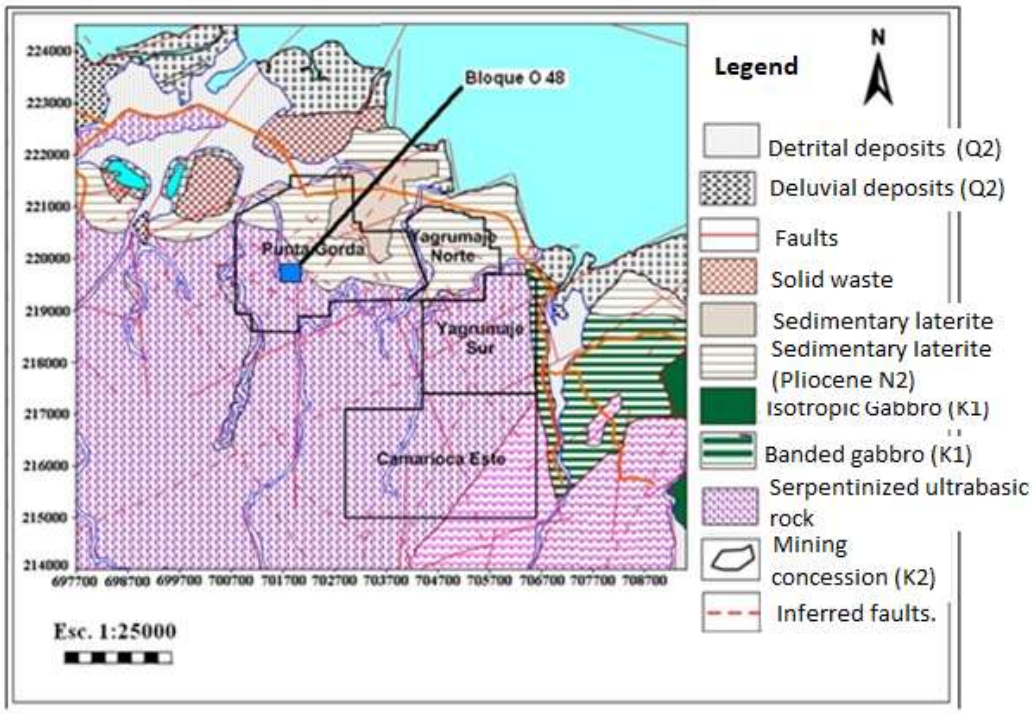

Figure 2. Geological map of the Punta Gorda deposit, from Guerásimov (1973) and modified after Fernández-Martínez (2020).

2.1. Materials

Samples (approximately 1 kg each) from the principal horizons of the weathering crust in sector O-48 were studied. The sampling targeted two types of lateritic profiles:

1. Profiles with the presence of white clayey material (P1, P2, and P5), designated as Clayey Lateritic Profiles (PLA) (Figure 3).

2. Profiles with horizons of light green (smectitic-chloritic) material (P3, P4, and P6), designated as Smectitic Lateritic Profiles (PLE) (Figure 4).

The Clayey Lateritic Profiles (PLA) exhibit saprolitic horizons with white clayey material and oxidized horizons, characteristic of laterites, with a yellowish to dark reddish-brown coloration. All these horizons possess low nickel content, as previously reported by Terrero-Reynosa (2010).

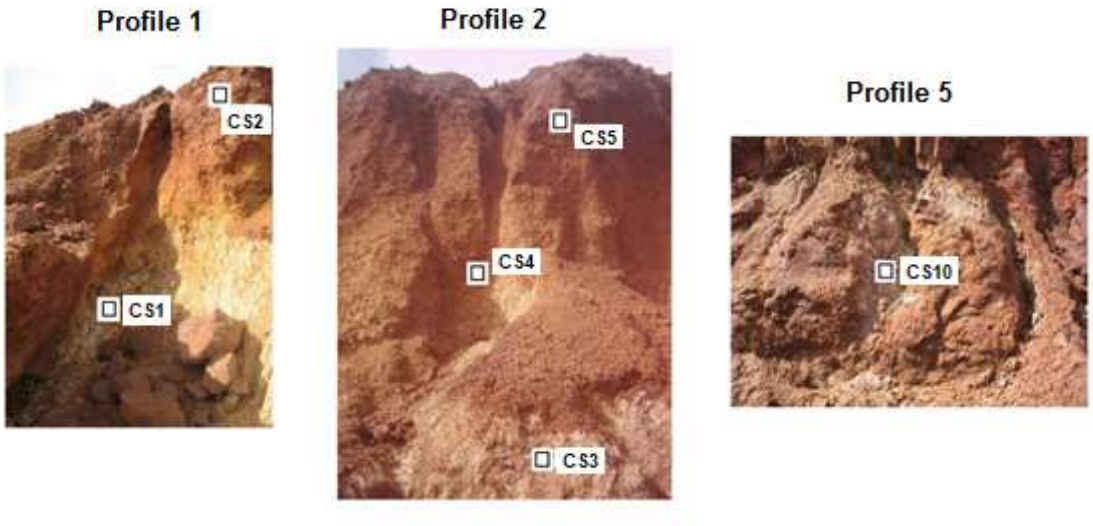

Figure 3. Clayey Lateritic Profiles from the O-48 sector of the Punta Gorda deposit. Sample collection points and their designations are indicated.

The Smectitic Lateritic Profiles (PLE) exhibit saprolitic horizons with light green material intermixed with red to reddish-brown ochers, situated within a setting of partially weathered rock materials associated with a fault zone. All these horizons possess a nickeliferous character, as reported by Terrero-Reynosa (2010).

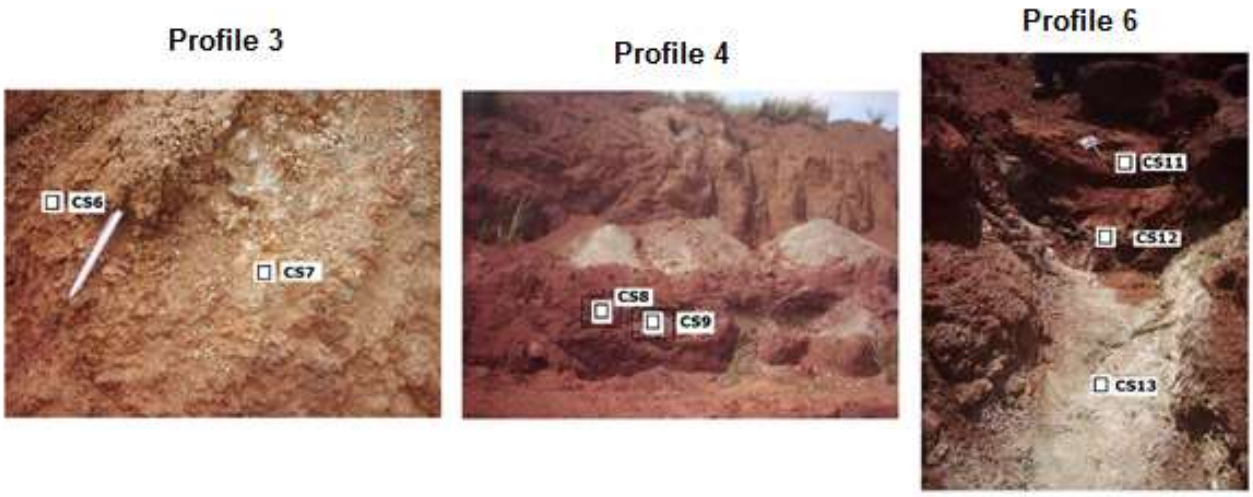

Figure 4. Smectitic Lateritic Profiles from the O-48 sector of the Punta Gorda deposit. Sample collection points and their designations are indicated.

2.2. Methods

Chemical analyses of the bulk samples were conducted at the laboratories of the Nickel Research Center (CEDINIQ) in Moa. Major elements (Mg, Si, Fe, Ni, Al, Co, Mn, and Cr) were determined using Inductively Coupled Plasma Atomic Emission Spectroscopy (ICP-AES).

The mineralogical determinations involved a preliminary reconnaissance stage to assess the most salient physical characteristics of the samples using standard Optical Microscopy. A TECHNIVAL binocular microscope, CARL ZEISS model AXIOLAB POL, was employed for this purpose.

The primary analytical technique used was X-Ray Diffraction (XRD), utilizing the powder method. The analysis was performed on a PHILIPS PW 3710 diffractometer at the Federal University of Pará, Brazil. The instrument was configured with Cu Kα and Co Kα radiation at 40 kV and 20 mA, using a Lynxeye detector. Data collection was carried out in a step-scan mode with a step size of 0.012° and a counting time of 96 seconds per step, over a 2θ range of 5° to 65°; for some samples, the range was extended to 5°–80°. Samples were homogenized and prepared according to the Bragg–Brentano method. Mineral identification was performed using X'Pert HighScore software (Degen *et al.*, 2014).

3. RESULTS

3.1. Chemical Characteristics of the Lateritic Profiles

The Clayey Lateritic Profiles (Table 1) exhibited high contents of silica and alumina, along with low levels of magnesium (up to 3.5%), iron (up to 8.5%),

and chromium (less than 0.85%) in their silicate (saprolitic) horizons. This chemical signature reflects the predominance of a clay component intermixed with a certain proportion of iron oxides (Figure 5).

Towards the upper section of these profiles, within the oxidized horizons, iron and aluminum oxides predominated, with some silica content. This is attributed to the presence of ferrous minerals containing a residual quantity of clays.

Table 1. Major element content in the Clayey Lateritic Profiles from the O-48 sector of the Punta Gorda deposit

Profile	Sample	Component/content (%)							
		NiO*	**CoO***	**Fe_2O_3**	**SiO_2**	**MgO**	**Cr_2O_3**	**MnO***	**Al_2O_3**
1	CS2	0,57	0,07	64,88	8,20	0,55	2,18	0,23	11,61
	CS1	0,69	0,02	5,57	36,80	3,44	0,85	0,01	20,13
2	CS5	0,48	0,07	51,87	8,80	0,51	3,13	0,36	18,33
	CS4	0,27	0,00	8,43	40,60	1,34	0,85	0,00	20,53
	CS3	0,36	0,00	4,86	39,70	1,27	0,63	0,00	22,27
5	CS10	0,60	0,00	2,86	41,80	2,74	0,47	0,03	21,66

*Includes the minor elements NiO, CoO, and MnO.

Three distinct saprolitic horizons are distinguished within the Smectitic-Chloritic Lateritic Profiles (Figure 5):

- Lower Saprolite: Characterized by high contents of silica (between 37% and 40%) and alumina (between 12% and 18%), along with moderate amounts of MgO (3.6% to 11.0%) and Fe_2O_3 (5% to 6%).
- Middle Saprolite: Marked by a Fe_2O_3 content of approximately 39%, SiO_2 ranging from 21% to 23%, and Al_2O_3 between 5% and 10%.
- Upper Saprolite: Defined by high contents of Fe_2O_3 (43.7% to 49.59%) and silica (16.20% to 23.0%), alongside MgO contents of 5.4% to 6.07% and approximately 6.0% alumina. This chemical assemblage evidences the presence of Mg-Al-Fe silicates intermixed with Fe oxides. Profile P6 (Table 2) exhibits the highest MgO contents (6.7% to 11.14%).

Table 2. Major element content in the Smectitic-Chloritic Lateritic Profiles from the O-48 sector of the Punta Gorda deposit

Profile	Sample	Component/content (%)							
		NiO*	CoO*	Fe_2O_3	SiO_2	MgO	Cr_2O_3	MnO*	Al_2O_3
3	CS7	1,46	0,05	39,15	21,20	7,19	2,35	0,25	10,70
	CS6	1,07	0,03	6,57	40,30	3,68	0,66	0,43	18,56
4	CS8	1,27	0,03	49,59	16,20	5,44	2,48	0,30	6,77
	CS9	1,37	0,02	6,29	37,40	6,33	0,75	0,12	17,04
6	CS11	1,20	0,03	43,73	23,00	6,07	2,35	0,25	6,20
	CS12	1,37	0,07	39,87	23,80	8,26	2,07	0,43	5,79
	CS13	1,59	0,05	5,14	40,00	11,14	0,61	0,15	12,52

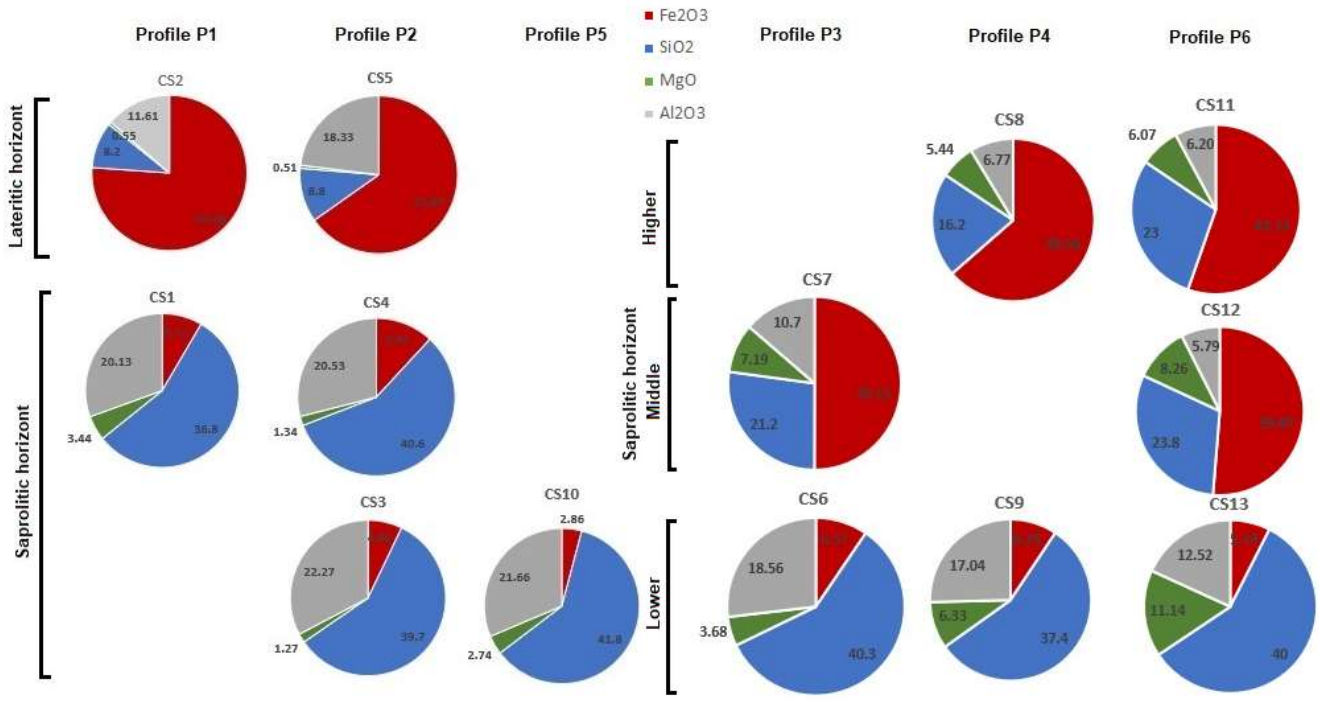

Figure 5. Graphical representation of the major element content (in wt.%)—Fe_2O_3, SiO_2, MgO, Al_2O_3—in samples from the lateritic profiles of the O-48 sector.

The NiO+MgO - Al_2O_3+Fe_2O_3 - SiO_2 ternary molar diagram for the Clayey Lateritic Profiles shows a clustered distribution of the clayey saprolitic samples (Figure 6A). These samples are characterized by an abundance of silica and alumina in their composition and a very low content of NiO+MgO (in a proportion of less than 10). The lateritic material in these profiles is

enriched in Al_2O_3+Fe_2O_3 but depleted in NiO+MgO, a geochemical behavior similar to that observed in deposits from the Philippines and Indonesia (Ito *et al.*, 2021; Aquino *et al.*, 2022).

The diagram for the Smectitic Profiles (Figure 6B) reveals a transitional trend in the composition of the saprolites. This trend progresses from a lower smectitic saprolitic horizon (samples CS13, CS9, and CS6), as confirmed by XRD results, to a middle, smectitic-chloritic horizon (samples CS7, CS11, and CS12), and finally to an upper, predominantly chloritic horizon (sample CS8).

The smectitic saprolites exhibit greater variability in magnesium and nickel content, alongside high silica levels (Figure 6B). In contrast, the chloritic saprolites possess a high proportion of Fe_2O_3 + Al_2O_3, which can reach approximately 60% or more, coupled with a lower silica content (20% to 30%).

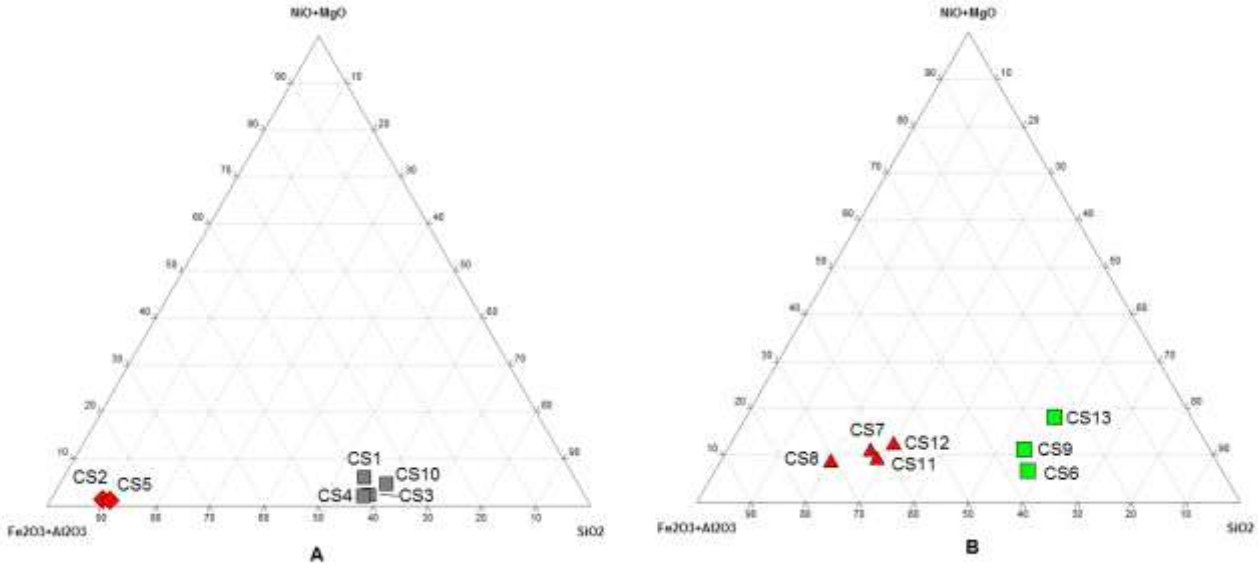

Figure 6. NiO+MgO - Al_2O_3+Fe_2O_3 - SiO_2 ternary molar diagram for samples from the O-48 sector of the Punta Gorda deposit. A) Kaolinitic Profiles. B) Smectitic Profiles.

3.2. Mineralogy of the Profiles

The Clayey (non-nickeliferous) Profiles exhibit distinctly kaolinitic saprolitic horizons (Figure 7), composed of a typical white material. In profiles P1 and P5, this material is intermixed with smectite and goethite, along with minor talc. In profile P2, kaolinite is associated with quartz, indicating siliceous mineralization.

The kaolinite-smectite-talc paragenesis suggests the existence of a weathered, lateral feldspathic body associated with a wedge of basic material rich in pyroxenes and magnesium phyllosilicates. Vertically, towards the lateritic horizon, the formation of Al oxyhydroxides is not observed; instead, the typical Fe oxides are present.

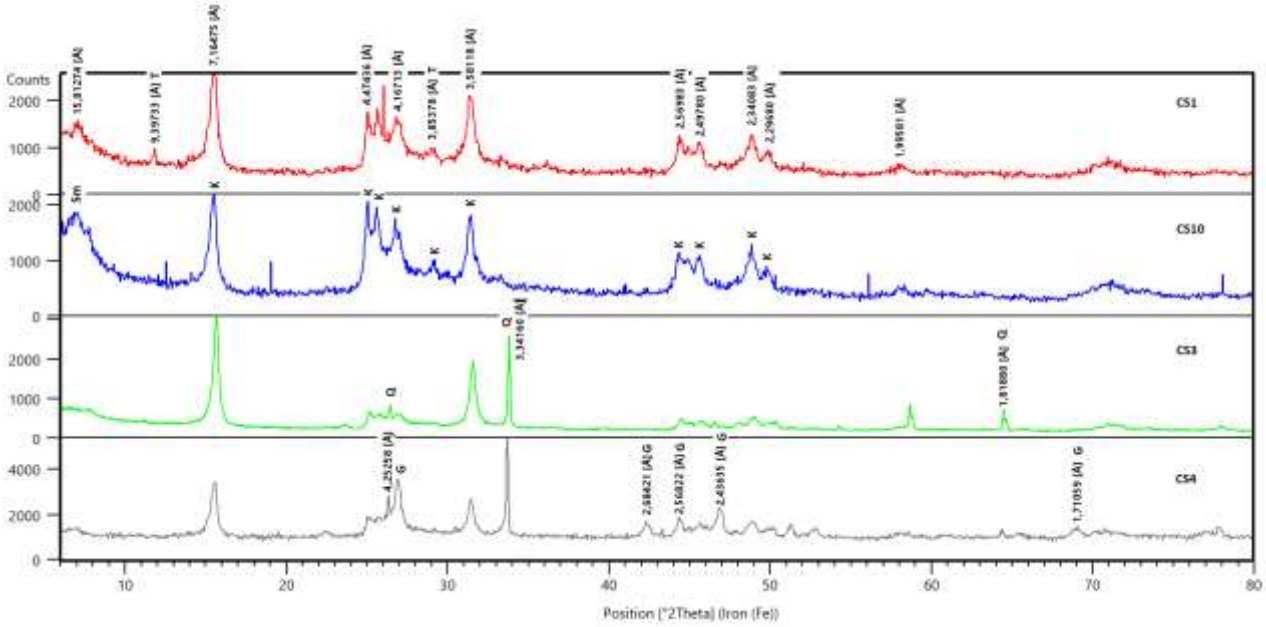

Figure 7. X-ray diffractograms of samples from the silicate horizon (CS1, CS10, CS3, CS4) of the non-nickeliferous kaolinitic profiles. Minerals: K: kaolinite; Sm: smectite; T: talc; G: goethita; Q: quartz.

The lateritic horizons are primarily composed of Fe oxides, predominantly goethite, along with hematite and maghemite, and a minor amount of kaolinite. The absence of gibbsite suggests an incomplete weathering process during clay formation.

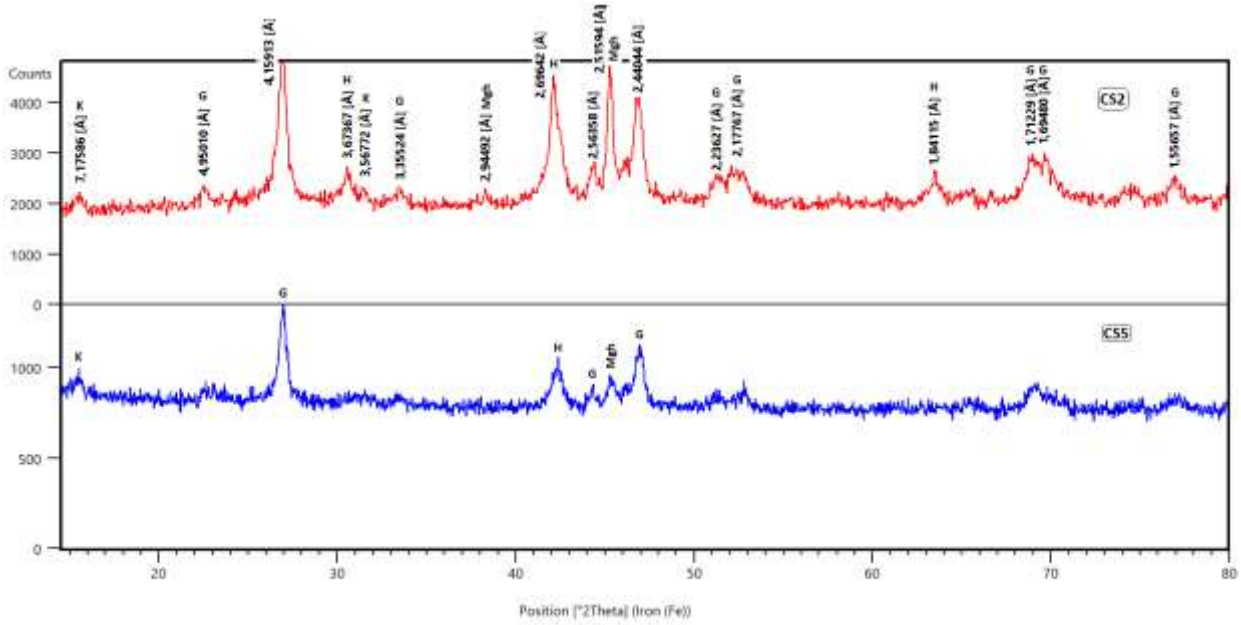

Figure 8. X-ray diffractograms of samples from the lateritic horizon (CS2, CS5) of the non-nickeliferous clayey profiles. Minerals: G: goethite; H: hematite; Mgh: maghemite; K: kaolinite.

Mineralogically, the Smectitic (nickeliferous) Profiles feature a distinctly smectitic lower saprolitic horizon, composed of a montmorillonite-type mineral ($(Mg, Ni)_xSi_4[Fe, Al, Mg, Ni]_{2-x}O_{10}(OH)_2$). This horizon exhibits a gradual transition to a nickeliferous clinochlore-pennine chlorite ($(Mg, Ni)_{3.75}Fe_{1.25}Si_3Al_2O_{10}(OH)_8$).

The gradational nature of this transition is most clearly observed in profile P6 (Figure 11). It is less evident in profile P3, which features an intermediate saprolite enriched in chlorite with minor smectite (sample CS7). In contrast, profile P4 exhibits a more abrupt transition (Figure 10) from the lower to the upper saprolite, with the latter dominated by chlorite (sample CS8) and devoid of smectite.

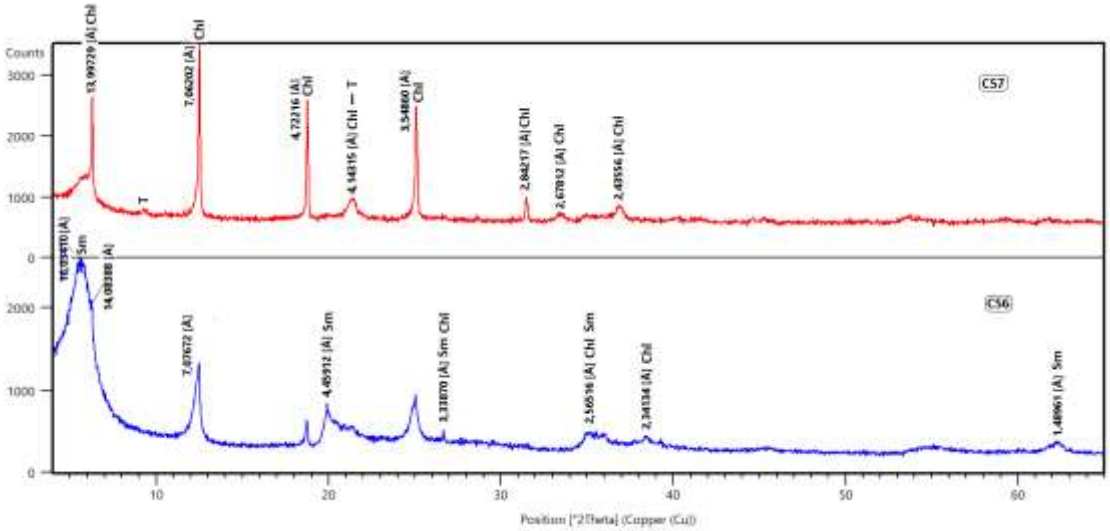

Figure 9. X-ray diffractograms of samples from the silicate horizon (CS7, CS6) of profile P3. Minerals: Chl: chlorite; T: talc; Sm: smectite (montmorillonite).

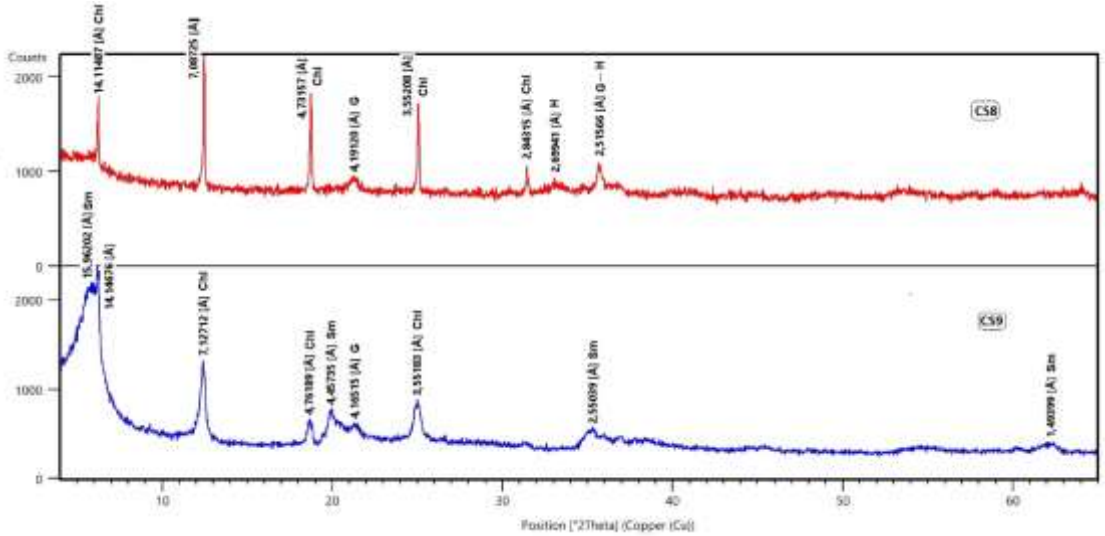

Figure 10. X-ray diffractograms of samples from the silicate horizon (CS8, CS9) of profile P4. Minerals: Sm: smectite (montmorillonite); Chl: chlorite; G: goethite; H: hematite.

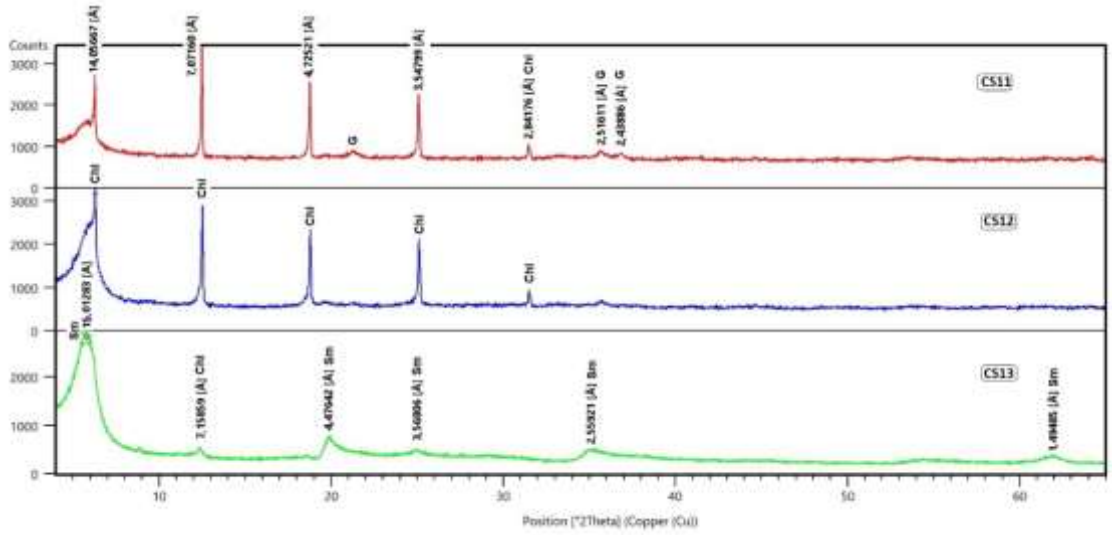

Figure 11. X-ray diffractograms of samples from the silicate horizon (CS11, CS12, CS13) of profile P6. Minerals: Sm: smectite (montmorillonite); Chl: chlorite; G: goethite.

4. DISCUSSION OF RESULTS

In the O-48 sector of the Punta Gorda deposit, profiles consisting of non-nickeliferous clayey horizons (less than 0.69% NiO) are found in association with profiles containing nickeliferous smectitic-chloritic horizons (between 1.07% and 1.59% NiO). For this deposit, which is frequently classified as an oxide-type deposit (Brand *et al.*, 1998; Oliveira *et al.*, 2001; Butt and Cluzel, 2013), the presence of these silicate-dominated profiles is atypical. This sector reveals four key aspects of interest:

- The presence of lateritic profiles with clayey and smectitic-chloritic saprolitic horizons within an oxide-type lateritic deposit.
- A well-differentiated distribution of nickel in the saprolitic horizons: the clayey (kaolinitic) horizons are nickel-poor (less than 0.69% NiO), whereas the smectitic-chloritic horizons are nickeliferous (1.07% to 1.59% NiO).
- The probable existence of a protolith composed of basic rocks with feldspathic intrusive bodies that, upon weathering, give rise to clays.
- The occurrence of a genetic transition between the smectitic and chloritic components.

Within the O-48 sector, the clayey lateritic profiles are located primarily in the eastern part (profiles P1, P2); P5 is situated more centrally, associated with a possible fault zone. In contrast, the nickeliferous smectitic-chloritic type (profiles P3, P4, P6) are located in the western part. This well-delimited

geographical distribution supports the assertion of the decisive influence of the bedrock type on the genesis of these saprolitic horizons.

Nickel is distributed in a highly differentiated manner in each of the profile types under study; the clayey profiles are distinctly non-nickeliferous, while the smectitic-chloritic profiles are nickeliferous. This allows for mineral beneficiation based on certain megascopic aspects (color, degree of compaction, among others) that could improve the quality of the nickeliferous ore feed supplied to the Caron process.

The existence of a protolith composed of basic rocks with feldspathic intrusive bodies that weather to clays is a subject requiring further development and validation with samples from these profiles. In this study, the genesis of kaolinite on one hand, and the chlorites on the other, has only been inferred based on the type of protolith from which they formed.

The clayey profiles exhibit a well-developed saprolitic horizon (essentially kaolinitic), with an estimated thickness of 1.5 m to 3 m. The kaolinite displays a complete diffractometric pattern (Figure 7), in which reflections from smectite (15.81 Å) and talc (9.39 Å) also appear. The presence of these latter two mineral phases suggests the existence of a mixture of peridotitic and harzburgitic rocks with gabbroic bodies in the O-48 sector of the Punta Gorda deposit. In the oxidized horizons of these profiles, certain amounts of clay mixed with iron oxides are present.

The genesis of kaolinite is justified by the mineralogical association produced during the weathering of the feldspathic component (basic plagioclase) within the gabbro body, according to the reaction:

$$\underset{\text{Plagioclase (Ca)}}{2Ca(Al_2Si_2O_8)} + 4H_2O \rightarrow \underset{\text{Kaolinite}}{Al_4(Si_4O_{10})(OH)_8} + 2CaO$$

This finding is supported by research results from Proenza *et al.* (1999) and Marchesi *et al.* (2006), who report the existence of gabbroic rocks intermixed with peridotites within the northeastern Cuban ophiolitic massif.

However, it is also probable that kaolinite formed from smectite (montmorillonite) through a diagenetic process (Putzolu *et al.*, 2020a; Putzolu *et al.*, 2020b). This is evidenced by the clear presence of the 15.81 Å diffractometric reflection attributable to smectite in the diffractograms of kaolinitic samples such as CS1 and CS10 (Figure 7). Furthermore, these samples possess a higher magnesium content among the saprolitic materials of these kaolinitic profiles.

Therefore, the presence of kaolinite in this context may have a dual origin: one through the weathering of a certain amount of feldspars (Ca-plagioclase), and another of diagenetic origin, proceeding from smectites (montmorillonite).

In the smectitic-chloritic profiles of Punta Gorda, a chemical distinction exists between the smectitic (Sm) and chloritic (Chl) saprolites. The former exhibit higher contents of silica (SiO_2) and alumina (Al_2O_3), with variable magnesium; whereas the chloritic saprolites are distinctly ferrous, with less silica and alumina, and a more stable magnesium content, as illustrated in Figure 12.

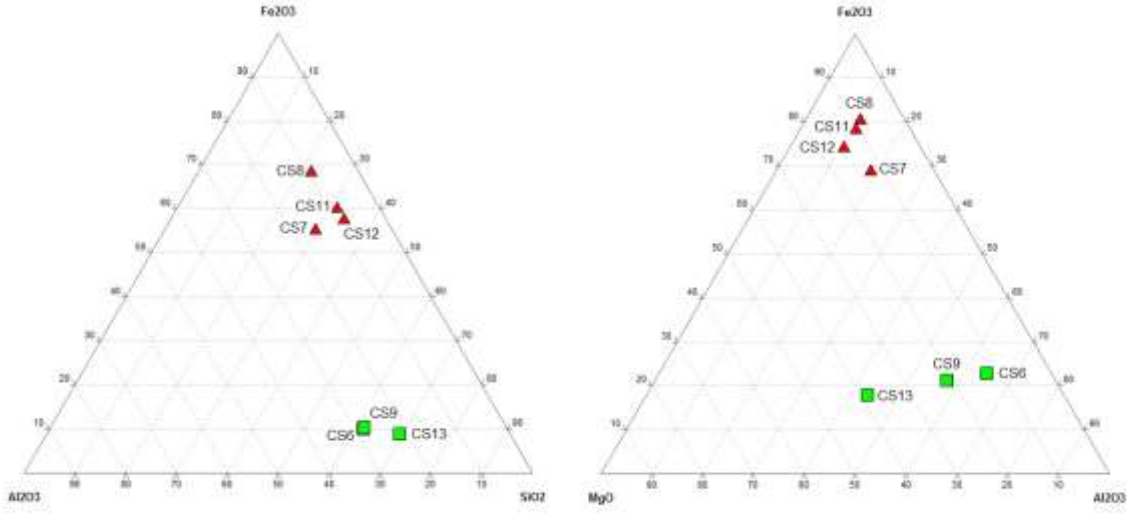

Figure 12. Ternary molar diagram of smectitic (CS6, CS9, CS13) and chloritic (CS7, CS8, CS11, CS12) saprolite samples from the O-48 sector of the Punta Gorda deposit.

The preceding evidence suggests that the process occurring in this case is the transformation of the smectitic component (Sm) to a chloritic component (Chl) through a process of progressive weathering, as previously described by various authors in other lateritic systems (Beaufort *et al.*, 1997; Murakami *et al.*, 1999; Gaudin *et al.*, 2005; Elert *et al.*, 2015; Meng *et al.*, 2018; Liu *et al.*, 2020). This interpretation is supported by the existence of chlorites with a significant iron content, higher than that of the smectitic component, as well as field observations (Figure 4) revealing a reddish, earthy chloritic material (characteristic of a supergenically altered product), which

collectively point towards a Sm to Chl transformation process via weathering in a lateritic system.

On the other hand, it is worth noting that regarding the smectite-chlorite (Sm-Chl) paragenesis in saprolitic horizons and its formation mechanism in these lateritic systems, there is no singular consensus. In addition to the model proposed by Gaudin *et al.* (2005), a different interpretation is presented by Putzolu *et al.* (2020b), who recognize the formation of smectite from chlorite (Chl → Sm) in a Ni lateritic system—a process that, until then, had only been acknowledged as common in regions where surface alteration affects metamorphic rocks (green schist facies).

For the mineralogy of the saprolitic horizon in the smectitic-chloritic profiles, it is useful to consider the findings of Gaudin *et al.* (2005), who distinguish two types of smectitic plasma in the saprolite zone. One is a Mg-rich smectite (saponite), previously reported by Camuti and Riel (1996) in the Murrin Murrin saprolite and commonly observed in other saprolites developed on ultrabasic rocks (Nahon *et al.*, 1982; Colin *et al.*, 1985; Yang & Shau, 1991). The second type of smectitic plasma is a dioctahedral Fe-rich smectite (Fe-nontronite, Fe-montmorillonite). Furthermore, these exhibit significant variations in Mg content: from $Fe(Cr)_{80}Mg(Ni)_{20}$ to $Fe(Cr)_{50}Mg(Ni)_{50}$, recognized as Fe-Mg smectites. Previously, iron-rich smectites in the saprolite zone had generally been described as nontronites (Besnus *et al.*, 1975; Nahon *et al.*, 1982).

We consider that the paragenesis detected in saprolite samples from the Punta Gorda deposit aligns with the model proposed by Gaudin *et al.* (2005) for Murrin Murrin. It is plausible that what actually exists are intermediate mineral phases between the dioctahedral smectite end-members (Fe-nontronite, Fe-montmorillonite) and the trioctahedral ones (Mg + Ni saponite).

5. CONCLUSIONS

- Within the Punta Gorda deposit, lateritic profiles composed of non-nickeliferous clayey horizons (containing less than 0.69% NiO) coexist with profiles featuring nickeliferous smectitic-chloritic horizons (between 1.07% and 1.59% NiO). This mineralogical zonation is atypical for a deposit classified as an oxide-type.

- The clayey profiles exhibit a well-developed, predominantly kaolinitic saprolitic horizon, forming a paragenesis with smectite and talc. The presence of kaolinite may have a dual origin: primarily from the

weathering of feldspars (Ca-plagioclase), and secondarily from a diagenetic alteration of smectites (montmorillonite).

- In Punta Gorda, smectitic (Sm) and chloritic (Chl) saprolites are chemically distinct. Smectitic saprolites display higher contents of silica (SiO_2) and alumina (Al_2O_3), with variable magnesium levels, whereas chloritic saprolites are distinctly ferrous, with lower silica and alumina, and a more homogeneous magnesium content.

- The smectite-chlorite (Sm-Chl) paragenesis in the saprolitic horizons is interpreted as the transformation of the smectitic component (Sm) to a chloritic component (Chl) through a process of progressive weathering within this lateritic system.

- The differentiated distribution of nickel between the non-nickeliferous clayey (kaolinitic) profiles and the nickeliferous smectitic profiles provides a basis for optimizing ore beneficiation strategies for the Caron process.

6. REFERENCES

Aiglsperger, T., Proenza, J. A., Lewis, J. F., Labrador, M., Svotjka, M., Rojas-Purón, A., Longo, F., & Ďurišová, J. (2016). Critical metals (REE, Sc, PGE) in Ni laterites from Cuba and the Dominican Republic. *Ore Geology Reviews*, *73*, 127-147. https://doi.org/10.1016/j.oregeorev.2015.10.010.

Altschuler, Z. S., Dwornik, E. J., & Kramer, J. (1963). Transformation of montmorillonite to kaolinite during weathering. *Science, 141*: 148–152.

Aquino, K. A., Arcilla, C. A., Schardt, C., & Tupaz, C. A. J. (2022). Mineralogical and Geochemical Characterization of the Sta. Cruz Nickel Laterite Deposit, Zambales, Philippines. Minerals 2022, 12, 305. https://doi.org/10.3390/min12030305.

Beaufort, D., Baronnet, A., Lanson, B., & Meunier, A. (1997). Corrensite: A single phase or a mixed-layer phyllosilicate in the saponite-to-chlorite conversion series? A case study of Sancerre-Couy deep drill hole (France). *American Mineralogist*, *82*, 109-124.

Besnus, Y., Fusil, G., Janot, C., Pinta, M. & Sieffermann, G. (1975). Characteristics of some weathering products of chromatic ultrabasic rocks in Bahia State, Brazil: nontronites, chlorites and chromiferous talc. In: Proceedings of the International Clay Conference (Mexico), pp. 27–34. Applied Publishing, Illinois.

Brand, N. W., Butt, C. R. M., & Elias, M. (1998). Nickel laterites: classification and features. *AGSO J Australian Geol Geoph, 17*, 81–88.

Butt, C. R. M., & Cluzel, D. (2013). Nickel laterite ore deposits: Weathered serpentinites. *Elements*, *9*, 123–128.

Camuti, K. S. & Riel, R. G. (1996). Mineralogy of the Murrin Murrin nickel laterites. In: Grimsey E. J. & Neuss I. eds. Nickel '96, Mineral to Market, pp. 209–210. Australasian Institute of Mining and Metallurgy Special Publication 6/96.

Colin, F., Noack, Y., Trescases, J. J. & Nahon, D. (1985). L'alte´ration late´ritique de´butante des pyroxe´nites de Jacuba, Niquelandia (Bresil). *Clay Minerals, 20*, 93–113.

Degen, T., Sadki, M., Bron, E., König, U., & Nénert, G. (2014). The HighScoresuite. *PowderDiffr, 29*, S13–S18.

Domenech, C., Galı, S., Villanova-de Benavent, C., Soler, J. M., & Proenza, J. A. (2017). Reactive transport model of the formation of oxide-type ni-laterite profiles (Punta Gorda, Moa Bay, Cuba). *Mineralium Deposita*, *52*(7), 993-1010.

Elert, K., Pardo, E. N., Rodriguez-Navarro, C. (2015). Mineralogical evolution of di- and trioctahedral smectites in highly alkaline environments. *Clays and Clay Minerals, 63*(6), 414–431.

Elias, M. (2002). *Nickel laterite deposits – a geological overview, resources and exploitation*. Centre for Ore Deposit Research, University of Tasmania, Hobart, Special Publication 4, pp 205-220.

Fernández-Martínez, L. (2020). *Modelo de la distribución espacial del material amenífero en la base minera de la Empresa del Níquel Ernesto Che Guevara.* Tesis Doctoral de la Universidad de Moa, Departamento de Geología. 100 p.

Freyssinet, P., Butt, C.R.M., Morris R.C., Piantone, P. (2005) Ore-forming processes related to lateritic weathering. In: Hedenquist JW, Thomson JFH, Goldfarb RJ, Richards JP (eds), *Economic Geology* 100th Anniversary Volume, 681-722.

Galí, S., Proenza, J. A., Labrador, M., Melgarejo, J. C., Tauler, E., Muñoz-Gómez, N., Rojas-Purón, A., & Orozco-Melgar, O. (2006). Caracterización mineralógica de los perfiles laterítico tipo óxido: yacimiento Punta Gorda (Cuba Oriental). *Macla, 6*, 197-199.

Gaudin, A., Decarreau, A., Noack, Y., & Grauby, O. (2005). Clay mineralogy of the nickel laterite ore developed from serpentinised peridotites at Murrin Murrin, Western Australia. *Australian Journal of Earth Sciences*, *52*, 231-241.

Gleeson, S. A., Butt, C. R. M., & Elias, M. (2003). Nickel laterites: A Review. *SEG Newsletter, 54*, 11-18.

Ito, A., Otake, T., Maulana, A., Sanematsu, K., Sufriadin, I.A. & Sato, T. (2021). Geochemical constraints on the mobilization of Ni and critical metals in laterite deposits, Sulawesi, Indonesia: A mass-balance approach. *Resource Geology,* 1–28. https://doi.org/10.1111/rge. 12266.

Iturralde-Vinent, M. (1996). Introduction to Cuban geology and geophysics. Ofiolitas y Arcos Volcánicos de Cuba. Miami, Florida. *Int. Geol. Correl. Programme, 364*, 3–35.

Lavaut-Copa, W. (1998). Tendencias geológicas del intemperismo de las rocas ultramáficas en Cuba oriental. *Minería y Geología, 15*, 9-16.

Lavaut-Copa, W. (2018). A Geological Classification for the Rocks of Weathering. *Petroleum Science and Engineering*, New York (USA), *2*(1), 1-6. doi: 10.11648/j.pse.20180201.11. ISSN: 2640-4516.

Liu, P., Wei, K., Chen, Z., Yuanzhi, T., Wancang, Z., Yuanfeng, C., Jingong, C., & Junfeng, J. (2020). Hydrothermal synthesis of chlorite from saponite: Mechanisms of smectite-chlorite conversion and influence of Mg2+ and Al3+ supplies. *Applied Clay Science*, *184*, 105357. ISSN 0169-1317.

Marchesi, C., Garrido, C. J., Godard, M., Proenza, J. A., Gervilla, F., & Blanco-Moreno, J. (2006). Petrogenesis of highly depleted peridotites and gabbroic rocks from the Mayarí-Baracoa Ophiolitic Belt (eastern Cuba). *Contributions to Mineralogy and Petrology*, *151*(6), 717-736.

Marsh, E. E. & Anderson, E. D. (2011). Ni–Co laterite deposits. U.S. Geological Survey, Open-File Report 2011, 1259, 1–9.

Meng, J., Xiaoyang, L., Benxian, L., Juncheng, Z., Daqian, H., Jiuhua, C., & Weiguang, S. (2018). Conversion reactions from dioctahedral smectite to trioctahedral chlorite and their structural simulations. *Applied Clay Science, 158,* 252-263. ISSN 0169-1317. https://doi.org/10.1016/j.clay.

Murakami, T., Sato, T. & Inoue, A. (1999). HRTEM evidence for the process and mechanism of saponite-to-chlorite conversion through corrensite.

American Mineralogist, 84(7-8), 1080-1087. https://doi.org/10.2138/am-1999-7-810

Nahon, D., Colin, F. & Tardy, Y. (1982). Formation and distribution of Mg, Fe, Mn-smectites in the first stages of the lateritic weathering of forsterite and tephroite. *Clay Minerals, 17*, 339–348.

Oliveira, S. M. B., de Moya-Partini, C. S., & Enzwelieler, J. (2001). Ochreous laterite: a nickel ore Punta Gorda, Cuba. *Journal South American Earth Science, 34*, 307–317. https://doi.org/10.1016/j.clay.2019.105357.

Proenza, J., Melgarejo, J., Gervilla, F., & Solé, J. (1999). Los niveles de gabros bandeados en el macizo ofiolitico Moa-Baracoa (Cuba); gabros característicos de cumulados de ofiolitas de zona de suprasubduccion. *Minería y Geología, 16*(12), 5-12.

Pushcharovsky, Y. (1988). Mapa geológico de la República de Cuba: Havana, Cuba/Moscow, USSR: Academy of Sciences of Cuba and Academy of Sciences of USSR, scale 1:250 000.

Putzolu, F., Abad, I., Balassone, G., Boni, M., & Mondillo, N. (2020b). Ni-bearing smectites in the Wingellina laterite deposit (Western Australia) at nanoscale: TEM-HRTEM evidences of the formation mechanisms. *Applied Clay Science*, *196*, 105753. ISSN 0169-1317. https://doi.org/10.1016/j.clay. 2020.105753.

Putzolu, F., Abad, I., Balassone, G., Boni, M., Cappelletti, P., Graziano, S. F., Maczurad, M., Mondillo, N., Najorka, J., & Santoro, L. (2020a). Parent rock and climatic evolution control on the genesis of Ni-bearing clays in Ni-Co laterites: New inferences from the Wingellina deposit (Western Australia). *Ore Geology Reviews, 120*.

Rojas-Purón, A., Rômulo-Simões, A., & Orozco-Melgar, G. (2012). Identificación mineralógica de los óxidos de manganeso del yacimiento laterítico Punta Gorda, Moa, Cuba. *Minería y Geología*, *28*(1), 1-26. ISSN 1993 8012.

Terrero-Reynosa, J. (2010). *Caracterización geoquímica y mineralógica del cuerpo silicatado en el sector septentrional del yacimiento Punta Gorda, Moa.* Tesis de maestría, Instituto Superior Minero Metalúrgico, Moa.

Yang, H. & Shau, Y. (1991). The altered ultramafic nodules from Mafu and Liutsu, Hsinchuhsien, Northern Taiwan with particular reference to the replacement of olivine and bronzite by saponite. *Special Publication of the Central Geological Survey*, *5*, 39–58.

Addicional Information

Conflict of Interest

The authors declare no conflicts of interest.

Author Contributions

ARP: Conceptualization of the presented mineralogical study, sampling and sample description, preparation of samples for chemical and XRD mineralogical determinations, drafting of the initial and final manuscript versions. **RSA**: Mineralogical determinations and interpretation of XRD data; review of the initial draft. **LFM**: Field reconnaissance and outcrop logging, sampling of the main sample collection, review of the final article. **ASM**: Mineralogical determinations and interpretation of XRD data, and definition of sample mineralogy.

ORCID

ALRP, https://orcid.org/0000-0002-9880-6744
RSA, https://orcid.org/0000-0002-3026-5523
LFM, https://orcid.org/0009-0005-7134-8500
ASM, https://orcid.org/0009-0003-4095-401X

Received: 15/09/2024
Accepted: 04/12/2024